PHYSICAL REVIEW A **103**, 053308 (2021)

Radial Fulde-Ferrell-Larkin-Ovchinnikov-like state in a population-imbalanced Fermi gas

Daisuke Inotani,[1,*] Shigehiro Yasui,[1,†] Takeshi Mizushima,[2,‡] and Muneto Nitta[1,§]

[1]*Department of Physics & Research and Education Center for Natural Sciences, Keio University, Hiyoshi 4-1-1, Yokohama, Kanagawa 223-8521, Japan*

[2]*Department of Materials Engineering Science, Osaka University, Toyonaka, Osaka 560-8531, Japan*

(Received 2 April 2021; accepted 16 April 2021; published 7 May 2021)

The possibility of a Fulde-Ferrell-Larkin-Ovchinnikov-like (FFLO-like) state in a population-imbalanced Fermi gas with a vortex is proposed. Employing the Bogoliubov-de Gennes formalism, we determine self-consistently the superfluid order parameter and the particle number density in the presence of a vortex. We find that, upon increasing the population imbalance, the superfluid order parameter spatially oscillates around the vortex core in the radial direction, indicating that the FFLO-like state becomes stable. We find that the radial FFLO-like states cover a wide region of the phase diagram in the weak-coupling regime at $T = 0$, in contrast with the conventional case without a vortex. We show that this inhomogeneous superfluidity can be detected as peak structures of the local polarization rate associated with the node structure of the superfluid order parameter. Since the vortex in the three-dimensional Fermi gas with population imbalance has been already realized in experiments, our proposal is a promising candidate of a FFLO-like state in cold atom physics.

DOI: 10.1103/PhysRevA.103.053308

I. INTRODUCTION

The Fulde-Ferrell-Larkin-Ovchinnikov (FFLO) states were proposed as inhomogeneous fermionic superfluids and superconductors with spatial oscillation of the order parameter [1,2]. The possibility of the FFLO states has been extensively discussed not only in condensed-matter physics such as superconductors [3–10] and ^{3}He under confinement [11–15] but also in high-energy physics such as high density QCD [16–18] and nuclear matter (proton superconductors and neutron superfluids) in a neutron star [19,20] and in a magnetar [21]. The FFLO states have been originally proposed as a ground state of superconductor with a Zeeman energy associated with magnetic field [1,2], but the realization of the FFLO state in electron system is still challenging, because the magnetic field causes orbital effects, which suppress the superconductivity, in addition to the Zeeman effects. Indeed, in the electron systems there are few promising candidates for the FFLO state. In the following, we simply refer to the "FFLO" state as a superfluidity where the order parameter spatially oscillates and its sign changes somewhere in the system, while in the original works [1,2] the FFLO states are characterized by the order parameter $\Delta(\boldsymbol{r})$ described by a plane wave as $\Delta(\boldsymbol{r}) = \Delta_0 e^{i\boldsymbol{q}\cdot\boldsymbol{r}}$ (FF state) and by a standing wave as $\Delta(\boldsymbol{r}) = \Delta_0 \cos(\boldsymbol{q}\cdot\boldsymbol{r})$ (LO state).

Ultracold Fermi gases have attracted much attention as an ideal system to realize the FFLO states both experimentally [22–27] and theoretically [28–42], because one can tune independently the Zeeman effects and the orbital effects. One of the most promising candidates is a one-dimensional (1D) Fermi gas with a population imbalance [37–40,43,44]. In this system, the FFLO state has been predicted to cover a large region of the phase diagram with respect to the interaction strength and population imbalance. Recently, the density profile of population imbalanced 1D Fermi gas was found to qualitatively agree with a theoretical prediction, exhibiting the FFLO state [26,27]. However, the evidence of the FFLO state has not been directly detected. Although it has been known that the FFLO state is also favored in two-dimensional (2D) systems [45], it has not been realized yet.

On the other hand, in the three-dimensional (3D) case, the realization of the FFLO state is still more challenging. In this case, it has been predicted that the FFLO states occupy only a narrow region in the phase diagram at zero temperature [28,32], and this region vanishes with increasing temperature [34] because the phase separation into a nonpolarized superfluid and a fully polarized normal fluid occurs. We note that, in the presence of the trapping potential, the spatial oscillation of the superfluid order parameter at the trap edge has been proposed within the Bogoliubov-de Gennes (BdG) formalism. However, because the amplitude of the oscillation is much smaller than the value of the superfluid order parameter in the bulk, it is difficult to detect. In Refs. [46,47], the angular-FFLO state, in which the superfluid order parameter oscillates in the angular direction of a toroidal trap, has been discussed. See also Ref. [48] for a FFLO state in a superconducting ring. Furthermore the FFLO state stabilized by an optical lattice has been proposed [49]. However, in both cases, any direct evidence of the FFLO state have not been observed, so far.

In this paper, we theoretically propose an experimentally accessible route to reach a FFLO-like state in 3D systems. In our idea, we consider a quantum vortex in the 3D superfluid Fermi gas with a population imbalance. In contrast with the case with no vortices, where the excess atoms gather at the

*dinotani@keio.jp
†yasuis@keio.jp
‡mizushima@mp.es.osaka-u.ac.jp
§nitta@phys-h.keio.ac.jp

trap edge, in the presence of a vortex, they can localize near the vortex core. As a result, the polarized Fermi gas is realized around the vortex core and a FFLO-like state appears in the wide region of the phase diagram with respect to the interaction strength and population imbalance at zero temperature. We emphasize that this situation should have already been experimentally realized [22,50], although the observation of the FFLO-like state has not been reported. Thus only a more precise measurement is needed to clearly detect the FFLO-like state. In this paper, we take $\hbar = k_{\rm B} = 1$.

II. FORMALISM

To clarify our idea we investigate a singly isolated quantum vortex in the two-component Fermi gas with population imbalance within the BdG formalism [51–53], starting from the Hamiltonian

$$H_{\rm BdG} = \sum_{\sigma=\uparrow,\downarrow}\int d\boldsymbol{r}\psi_\sigma^\dagger(\boldsymbol{r})\left(-\frac{\nabla^2}{2m}-\mu_\sigma\right)\psi_\sigma(\boldsymbol{r}) + \int d\boldsymbol{r}(\Delta(\boldsymbol{r})\psi_\uparrow^\dagger(\boldsymbol{r})\psi_\downarrow^\dagger(\boldsymbol{r}) + {\rm H.c.}) - U_s\sum_{\sigma=\uparrow,\downarrow}\int d\boldsymbol{r}n_{-\sigma}(\boldsymbol{r})\psi_\sigma^\dagger(\boldsymbol{r})\psi_\sigma(\boldsymbol{r}). \quad (1)$$

Here $\psi_\sigma(\boldsymbol{r})$ is the field operator of a Fermi atom with pseudospin $\sigma = \uparrow,\downarrow$ and atomic mass m. μ_σ is the chemical potential of the σ component. The population imbalance is included in the difference between $\mu_\uparrow$ and $\mu_\downarrow$. The second and third terms describe the contribution from the superfluid order parameter $\Delta(\boldsymbol{r}) = -U_s\langle\psi_\downarrow(\boldsymbol{r})\psi_\uparrow(\boldsymbol{r})\rangle$ and the Hartree potential $-U_s n_{-\sigma}(r) = -U_s\langle\psi_{-\sigma}^\dagger(\boldsymbol{r})\psi_{-\sigma}(\boldsymbol{r})\rangle$, respectively, where $n_\sigma(\boldsymbol{r})$ is the number density of the σ component.

We consider a single vortex along the z axis with the winding number $w = 1$ at $\rho = 0$ in the cylindrical coordinates $\boldsymbol{r} = (\rho,\theta,z)$. In this cylindrically symmetric situation, we can write the superfluid order parameter and particle number density as $\Delta(\boldsymbol{r}) = \Delta(\rho)e^{i\theta}$ and $n_\sigma(\boldsymbol{r}) = n_\sigma(\rho)$, respectively. In this paper, we consider the FFLO state with a spatial oscillation of $\Delta(\rho)$ along the radial direction.

The mean fields, i.e., $\Delta(\rho)$ and $n_\sigma(\rho)$, as well as the chemical potential μ_σ, are determined self-consistently by solving the gap equation and the particle number equations for a given interaction strength and population imbalance $P = (N_\uparrow - N_\downarrow)/(N_\uparrow + N_\downarrow)$, where $N_\sigma = \int d\boldsymbol{r}n_\sigma(\boldsymbol{r})$ is the total atomic number of the σ component. This procedure can be achieved by conventional diagonalization, i.e., the Bogoliubov transformation for a finite-size system having the cylindrical symmetry with the system radius R ($0 \leqslant \rho \leqslant R$) and height L ($0 \leqslant z \leqslant L$).[1] In addition to $\Delta(\rho)$ and $n_\sigma(\rho)$, we calculate the local density of states (LDOS) given by

$$\mathcal{N}_\uparrow(\omega,\rho) = -\frac{1}{\pi}{\rm Im}G_{11}(\boldsymbol{r},\boldsymbol{r},i\omega_n \to \omega + i\epsilon), \quad (2)$$

$$\mathcal{N}_\downarrow(\omega,\rho) = \frac{1}{\pi}{\rm Im}G_{22}(\boldsymbol{r},\boldsymbol{r},i\omega_n \to \omega + i\epsilon), \quad (3)$$

[1]See Appendix for the details of the calculations.

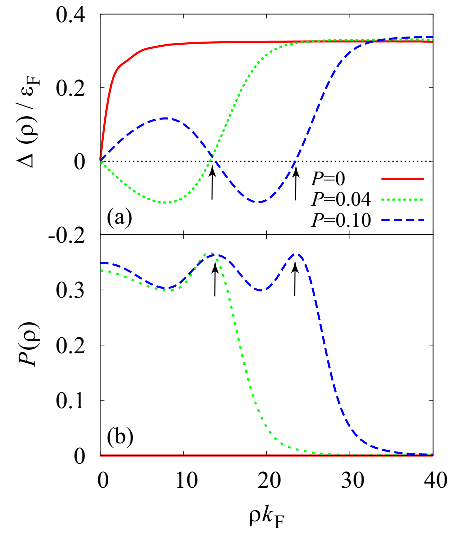

FIG. 1. Calculated (a) superfluid order parameter and (b) local population imbalance $P(\rho) = [n_\uparrow(\rho) - n_\downarrow(\rho)]/[n_\uparrow(\rho) + n_\downarrow(\rho)]$, as a function of ρ. The solid line shows the results with $P = 0$. The dotted and dashed line are corresponding the case with $N = 1$ and $N = 2$, respectively, where N is the number of the node structure. In this figure we take $(k_{\rm F}a_s)^{-1} = -0.5$. The arrows denote the node structure in the case with $N = 2$ (dashed line).

where $\omega_n = (2n+1)\pi T$ ($n \in \mathbb{Z}$) is the Matsubara frequency at temperature T, and ϵ is an infinitesimally small parameter. Here

$$\hat{G}(\boldsymbol{r},\boldsymbol{r}',i\omega_n) = -\int_0^\beta e^{i\omega_n\tau}\langle T_\tau\{\Psi(\boldsymbol{r},\tau),\Psi^\dagger(\boldsymbol{r}',0)\}\rangle d\tau \quad (4)$$

is a 2×2 single-particle Green's function with the two-component Nambu-Gor'kov field operator $\Psi(\boldsymbol{r},\tau) = (\psi_\uparrow(\boldsymbol{r},\tau)\psi_\downarrow^\dagger(\boldsymbol{r},\tau))$. Finally, we summarize the setup of the numerical calculations. We take $Rk_{\rm F} = 50$ and $Lk_{\rm F} = 20$ for the system size of the ρ and z directions, respectively, where $k_{\rm F}$ is the Fermi momentum. We take the cutoff energy $E_c = 9\varepsilon_{\rm F}$ with the Fermi energy $\varepsilon_{\rm F} = k_{\rm F}^2/(2m)$. We fix $T = 0$.

III. RESULTS

In Fig. 1, we show the self-consistent solutions of $\Delta(\rho)$ in the weak-coupling regime with $(k_{\rm F}a_s)^{-1} = -0.5$, where a_s is the s-wave scattering length.[2] In the absence of the population imbalance ($P = 0$), the ordinary vortex is obtained. As P increases, we find that $\Delta(\rho)$ spatially oscillates around the vortex core and approaches the value in the bulk away from the vortex core, which indicates a FFLO-like state is locally realized near the vortex core. Here, we note that the superfluid order parameter oscillates in the ρ direction. Thus, the rotational symmetry around the vortex core remains in this solution, in contrast with the original FF and LO states. Further increasing P, the number N of nodes [where $\Delta(\rho) = 0$] increases. The dotted and dashed lines in Fig. 1(a) correspond to the $N = 1$ and $N = 2$ cases, respectively. Here, we

[2]See Appendix for the definition of a_s.

comment on the effects of trapping potential, which is not explicitly considered in this work. The system size of cold atomic gases is typically about $100k_F^{-1}$–$1000k_F^{-1}$, which is much longer than the vortex size obtained in our calculation ($\approx 10k_F^{-1}$, as shown in Fig. 1). Thus, one can neglect the effects of trapping potential as long as one focuses on the physics around the vortex core.

This dependence of $\Delta(\rho)$ on P can be understood as follows: In the presence of the population imbalance, the excess atoms gather into the region where the superfluid order parameter is small, because the excess atoms feel the superfluid order parameter as a potential. The sign change of the superfluid order parameter at vortices and FFLO nodal planes leads to the formation of low-lying quasiparticle states. Bogoliubov quasiparticle states in the vortex core are discretized to the Caroli-de Gennes-Matricon (CdGM) states with level spacing $\approx \Delta_0^2/\varepsilon_F$, where Δ_0 is the bulk value of the superfluid order parameter [54,55], while the FFLO nodal planes are accompanied by midgap Andreev bound states [56–58]. When the population imbalance is small, the excess atoms are accumulated by the CdGM states and thus localize around the vortex core. However, upon increasing the number of excess atoms, the vortex size also increases to contain more atoms, leading to the increase of energy of the vortex. Eventually, it becomes energetically favorable to make a node structure, which is accompanied by midgap Andreev bound states and can accumulate the excess atoms. Hence, the existence of a vortex line can become a trigger for realizing the FFLO-like state. Indeed, as shown in Fig. 1(b), the local polarization rate defined by $P(\rho) = [n_\uparrow(\rho) - n_\downarrow(\rho)]/[n_\uparrow(\rho) + n_\downarrow(\rho)]$ has peak structures around the nodes [$\rho k_F \simeq 13, 24$ for the dashed line in Fig. 1(b)], which can be measured as evidence of our proposal.

We also emphasize that the amplitude of the oscillation of $\Delta(\rho)$ is comparable to the bulk value of the superfluid order parameter. This is in contrast with the trapped case, where, although the similar oscillation is predicted at the trap edge, the amplitude is much smaller than the value of $\Delta(\boldsymbol{r})$ at the trap center [35]. The resultant local polarization cannot possess pronounced peak structures at the nodal planes. Thus, the FFLO-like state proposed in this work is more promising to experimentally detect.

The spatial structure of the superfluid order parameter $\Delta(\boldsymbol{r}) = \Delta(\rho)e^{i\theta}$ is shown in Fig. 2. We find the clear oscillation of $\Delta(\boldsymbol{r})$ in the radial direction ρ. In addition to these nodes, the real (imaginary) part of $\Delta(\boldsymbol{r})$ vanishes along the y (x) axis. This is simply because of the phase factor $e^{i\theta}$ associated with the vortex.

The midgap Andreev bound states and the CdGM states, which are associated with the nodal planes of the FFLO-like state and the vortex, respectively, can be detected by an observation of the LDOS $\mathcal{N}_\sigma(\omega, \rho)$. Figure 3 shows the calculated LDOS with the same parameters as in the case with $N = 2$ in Fig. 1 (dashed lines). While in the bulk region the clear gap structure opens in LDOS, in the region where the superfluid order parameter spatially oscillates ($\rho k_F \lesssim 30$), LDOS has a finite value with an energy inside the superfluid gap. To clearly see this, in the lower panels in Fig. 3, we show the ρ dependence of LDOS with a fixed energy ($\omega = -0.16\varepsilon_F$ for ↑ spin and $\omega = 0.28\varepsilon_F$ for ↓ spin). In each panel, we find

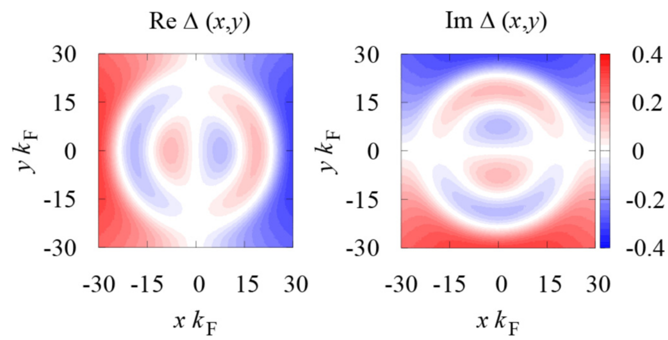

FIG. 2. Spatial structure of the superfluid order parameter $\Delta(\boldsymbol{r}) = \Delta(\rho)e^{i\theta}$ in the x-y plane. The parameters are taken to be the same as those in the $N = 2$ case in Fig. 1.

three peak structures. The peak around the vortex core $\rho \simeq 0$ corresponds to the CdGM states, and the others correspond to the midgap Andreev bound states. Thus, the disappearance of the gap structure in LDOS except around the vortex core can be evidence of the realization of a FFLO-like state. Since the occupied LDOS can be experimentally observed by using local photoemission spectroscopy [59], the characteristic structures in the LDOS of the ↑ component are accessible.

Finally, we show the phase diagram with respect to $(k_F a_s)^{-1}$ and P at $T = 0$ in Fig. 4. We find that the FFLO state covers a wide region of the phase diagram in the weak-coupling regime $(k_F a_s)^{-1} \leqslant 0$ in contrast with the conventional superfluid phase *without* the spatial oscillation of $\Delta(\boldsymbol{r})$, which is realized only in the case with small population imbalance.

We also mention that, as one goes into the strong-coupling regime where $(k_F a_s)^{-1} > 0$, the FFLO-like state continuously

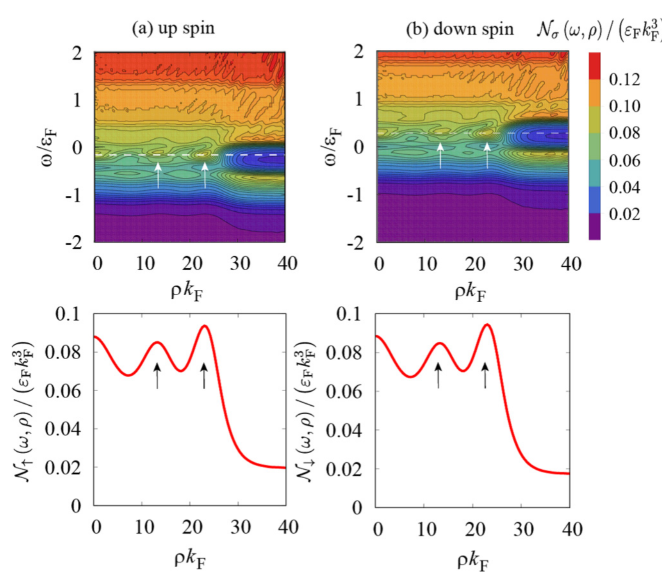

FIG. 3. Calculated LDOS of the (a) ↑ and (b) ↓ components (upper panels). The parameters are taken to be the same as those in the $N = 2$ case in Fig. 1. Values of LDOS along the dashed lines in upper panels are also shown (lower panels). We use $\omega = -0.16\varepsilon_F$ for ↑ spin and at $\omega = 0.24\varepsilon_F$ for ↓ spin. The arrows indicate the midgap Andreev states around the nodal planes of the FFLO state.

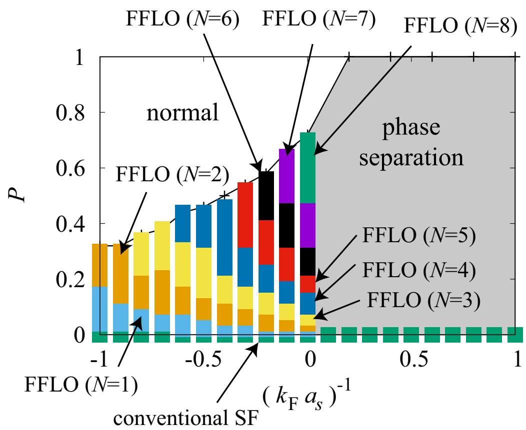

FIG. 4. Phase diagram of the population imbalanced Fermi gas with a vortex. N in the FFLO state denotes the number of the node structure. In the shaded area in the strong-coupling regime, the phase separation into the nonpolarized superfluid and the fully polarized normal fluid occurs. The conventional superfluid (SF) state without spatial oscillation of the superfluid order parameter is obtained only in the absence of the population imbalance $P = 0$ within our calculation.

changes into the phase-separated state between the strongly polarized region around the vortex core and the spin-balanced superfluid region, which happens in the trapped case without a vortex. Since the FFLO-like state is stabilized by the mismatch of the size of the Fermi surface between the $\uparrow$ and $\downarrow$ components, in the spin-balanced superfluid region, the FFLO oscillation cannot be realized. On the other hand, in the strongly polarized region around the vortex core, since the local polarization rate P almost reaches unity, the superfluid order parameter itself is strongly suppressed. Thus, the FFLO-like state is favored in the weak-coupling regime. The phase boundary between the FFLO-like and phase-separated states cannot be defined because the FFLO-like state continuously changes into the phase-separated state as increasing the interaction strength. However, within our calculation, we cannot find the FFLO-like solution in the region where $(k_F a_s)^{-1} \geqslant 0.1$.

IV. SUMMARY

To summarize, we have proposed a route to reach a FFLO-like superfluid in a 3D Fermi gas. We have considered a population-imbalanced Fermi gas with a vortex. Applying the BdG formalism to this system, we have shown that the spatial oscillation of the superfluid order parameter appears near the vortex core and the number of the node structure increases as the population imbalance increases. We have also found that the FFLO nature can be seen as peak structures in the local polarization rate, as well as vanishing gap structure in the LDOS. We have shown that the FFLO-like states cover a wide region of the phase diagram in the weak-coupling regime at zero temperature in contrast to the conventional case without a vortex.

Finally, we comment on the effects of fluctuations on the FFLO-like state. It has been reported that the ordinary FFLO state is strongly suppressed by the phase fluctuations of the order parameter in a uniform three-dimensional system [60,61]. Since in the FFLO-like state discussed in this paper the spatial oscillation of the order parameter appears locally around the vortex core, in contrast with the ordinary FFLO states, it is still an open question how the fluctuations affect the FFLO-like state in our situation. Therefore, we leave this as a future problem.

ACKNOWLEDGMENTS

This work is supported by the Ministry of Education, Culture, Sports, Science (MEXT)-Supported Program for the Strategic Research Foundation at Private Universities "Topological Science" (Grant No. S1511006). This work is also supported in part by the Japan Society for the Promotion of Science (JSPS) Grants-in-Aid for Scientific Research [KAKENHI Grants No. 17K05435 (S.Y.), No. JP16K05448 (T.M.), No. JP20K03860 (T.M), JP20H01857 (T.M.), No. 16H03984 (M.N.), and No. 18H01217 (M.N.)], and also by MEXT KAKENHI Grant-in-Aid for Scientific Research on Innovative Areas "Topological Materials Science," Grant No. 15H05855 (T.M. and M.N.), and "Quantum Liquid Crystals" No. JP20H05163 (T.M.).

APPENDIX: DIAGONALIZATION OF THE BOGOLIUBOV-DE GENNES HAMILTONIAN IN CYLINDRICAL SYSTEM

In this section, we summarize the procedure of the diagonalization of the BdG Hamiltonian in Eq. (1) under the cylindrical symmetry. For this purpose, it is useful to expand $\psi_\sigma(\boldsymbol{r})$ with respect to a set of eigenfunctions of the kinetic-energy term in the cylindrical coordinate as

$$\psi_\sigma(\boldsymbol{r}) = \sum_{j=1}^{\infty} \sum_{l=-\infty}^{\infty} \sum_{k_z} c_{j,\sigma}^{l,k_z} f_{j,l,k_z}(\boldsymbol{r}), \tag{A1}$$

where

$$f_{j,l,k_z}(\boldsymbol{r}) = \phi_{j,l}(\rho) e^{il\theta} \frac{e^{ik_z z}}{\sqrt{2\pi L}}. \tag{A2}$$

Here L is the height to the z direction of the system ($0 \leqslant z \leqslant L$), $k_z = 2\pi n_z/L$ ($n_z \in \mathbb{Z}$), and the normalized radial wave function $\phi_{j,l}(\rho)$ is given by

$$\phi_{j,l}(\rho) = \frac{\sqrt{2}}{R J_{l+1}(\alpha_{j,l})} J_l\left(\alpha_{j,l}\frac{\rho}{R}\right), \tag{A3}$$

where J_l is Bessel function, $\alpha_{j,l}$ is the jth zero of J_l, and R is the system radius ($0 \leqslant \rho \leqslant R$). In this basis, the BdG Hamiltonian in Eq. (1) can be written as

$$H_{\rm BdG} = \sum_{l,k_z} \sum_{j,j'} \Phi_j^{l,k_z\dagger} h_{j,j'}^{l,k_z} \Phi_{j'}^{l,k_z}. \tag{A4}$$

Here, we have introduced the Nambu-Gor'kov field operator in the cylindrical coordinate as

$$\Phi_j^{j,k_z} = \begin{pmatrix} c_{j,\uparrow}^{l,k_z} \\ c_{j,\downarrow}^{-l-1,-k_z\dagger} \end{pmatrix}, \tag{A5}$$

$$\Phi_j^{j,k_z\dagger} = \begin{pmatrix} c_{j,\uparrow}^{l,k_z\dagger} & c_{j,\downarrow}^{-l-1,-k_z} \end{pmatrix}, \tag{A6}$$

and the matrix $h^{l,k_z}_{j,j'}$ is given by

$$h^{l,k_z}_{j,j'} = \begin{pmatrix} \xi^{\uparrow}_{j,l,k_z}\delta_{j,j'} + F^{l,\uparrow}_{j,j'} & \Delta^{l}_{j,j'} \\ \Delta^{l}_{j,j'} & -\xi^{\downarrow}_{j,l+1,k_z}\delta_{j,j'} - F^{l+1,\downarrow}_{j,j'} \end{pmatrix}, \quad \text{(A7)}$$

with the superfluid order parameter

$$\Delta^{l}_{j,j'} = \int_0^R \rho d\rho \phi_{j,l}(\rho)\Delta(\rho)\phi_{j',l+1}(\rho), \quad \text{(A8)}$$

and the Hartree potential

$$F^{l,\sigma}_{j,j'} = -U_s \int_0^R \rho d\rho \phi_{j,l}(\rho) n_{-\sigma}(\rho)\phi_{j',l}(\rho). \quad \text{(A9)}$$

The Hamiltonian can be diagonalized by the Bogoliubov-Valatin transformation,

$$\gamma^{l,k_z}_{j,\sigma} = \sum_{j',\sigma'} (W^{-1})^{l,k_z}_{\{j,\sigma\},\{j',\sigma'\}} \Phi^{l,k_z}_{j',\sigma'}, \quad \text{(A10)}$$

with an orthogonal matrix $\hat{W}$ as

$$H_{\rm BdG} = \sum_{\sigma} \sum_{j,l,k_z} E^{l,k_z}_{j,\sigma} \left(\gamma^{l,k_z}_{j,\sigma}\right)^{\dagger} \gamma^{l,k_z}_{j,\sigma}, \quad \text{(A11)}$$

where $E^{l,k_z}_{j,\sigma}$ are the eigenvalues of the Hamiltonian. We note that the matrix in the original BdG Hamiltonian in Eq. (1) is diagonal in terms of l and k_z. Thus, it is sufficient to numerically solve the eigenvalue equation with l and k_z fixed.

Using the set of eigenfunction W and eigenvalues E, the self-consistent equations for the superfluid order parameter and the particle number density can be obtained as

$$\Delta(\boldsymbol{r}) = -\frac{U_s e^{-i\theta}}{2\pi L} \sum_{l,k_z} \sum_{j,j'} \phi_{j,l+1}(\rho)\phi_{j',l}(\rho) d^{l,k_z}_{j,j'}, \quad \text{(A12)}$$

$$n_{\uparrow}(\boldsymbol{r}) = \frac{1}{2\pi L} \sum_{l,k_z} \sum_{j,j'} \phi_{j,l}(\rho)\phi_{j',l}(\rho)\eta^{\uparrow}_{j,j'}, \quad \text{(A13)}$$

$$n_{\downarrow}(\boldsymbol{r}) = \frac{1}{2\pi L} \sum_{l,k_z} \sum_{j,j'} \phi_{j,l+1}(\rho)\phi_{j',l+1}(\rho)\eta^{\downarrow}_{j,j'}, \quad \text{(A14)}$$

respectively. Here, we have defined

$$d^{l,k_z}_{j,j'} = \sum_{i,\sigma} W^{l,k_z}_{\{j,\downarrow\},\{i,\sigma\}} W^{l,k_z}_{\{j',\uparrow\},\{i,\sigma\}} n_{\rm F}\left(E^{l,k_z}_{i,\sigma}\right), \quad \text{(A15)}$$

$$\eta^{\uparrow}_{j,j'} = \sum_{i,\sigma} W^{l,k_z}_{\{j,\uparrow\},\{i,\sigma\}} W^{l,k_z}_{\{j',\uparrow\},\{i,\sigma\}} n_{\rm F}\left(E^{l,k_z}_{i,\sigma}\right), \quad \text{(A16)}$$

$$\eta^{\downarrow}_{j,j'} = \sum_{i,\sigma} W^{l,k_z}_{\{j,\downarrow\},\{i,\sigma\}} W^{l,k_z}_{\{j',\downarrow\},\{i,\sigma\}} \left[1 - n_{\rm F}\left(E^{l,k_z}_{i,\sigma}\right)\right]. \quad \text{(A17)}$$

To avoid the well-known ultraviolet divergence, we need to introduce a cutoff energy $E_{\rm c}$ in the gap equation. We also note that the interaction strength is conveniently measured by the s-wave scattering length a_s in cold atom physics. In the cylindrical system, a_s is known to be related to the coupling constant U_s and the cutoff energy $E_{\rm c}$ as [35,62]

$$\frac{1}{k_{\rm F}a_s} = -\frac{8\pi\varepsilon_{\rm F}}{U_s k_{\rm F}^3} + \frac{2}{\pi}\sqrt{\frac{E_{\rm c}}{\varepsilon_{\rm F}}}. \quad \text{(A18)}$$

Using the Bogoliubov-Valatin transformation (A10) and the eigenfunctions $f_{j,l,k_z}(\boldsymbol{r})$, we can write the matrix element of the single-particle Green's function $G_{ij}(\boldsymbol{r},\boldsymbol{r}',i\omega_n)$, which is defined by Eq. (4), as

$$G_{11}(\boldsymbol{r},\boldsymbol{r}',i\omega_n) = \sum_{j,j'}\sum_{l,k_z}\sum_{i,\sigma} \frac{W^{l,k_z}_{\{j,\uparrow\},\{i,\sigma\}} W^{l,k_z}_{\{j',\uparrow\},\{i,\sigma\}}}{i\omega_n - E^{l,k_z}_{i,\sigma}} \times f_{j,l,k_z}(\boldsymbol{r}) f^{*}_{j',l,k_z}(\boldsymbol{r}'), \quad \text{(A19)}$$

$$G_{22}(\boldsymbol{r},\boldsymbol{r}',i\omega_n) = \sum_{j,j'}\sum_{l,k_z}\sum_{i,\sigma} \frac{W^{l,k_z}_{\{j,\downarrow\},\{i,\sigma\}} W^{l,k_z}_{\{j',\downarrow\},\{i,\sigma\}}}{i\omega_n - E^{l,k_z}_{i,\sigma}} \times f^{*}_{j,-l-1,-k_z}(\boldsymbol{r}) f_{j',-l-1,-k_z}(\boldsymbol{r}'), \quad \text{(A20)}$$

$$G_{12}(\boldsymbol{r},\boldsymbol{r}',i\omega_n) = \sum_{j,j'}\sum_{l,k_z}\sum_{i,\sigma} \frac{W^{l,k_z}_{\{j,\uparrow\},\{i,\sigma\}} W^{l,k_z}_{\{j',\downarrow\},\{i,\sigma\}}}{i\omega_n - E^{l,k_z}_{i,\sigma}} \times f_{j,l,k_z}(\boldsymbol{r}) f_{j',-l-1,-k_z}(\boldsymbol{r}'), \quad \text{(A21)}$$

$$G_{21}(\boldsymbol{r},\boldsymbol{r}',i\omega_n) = G^{*}_{12}(\boldsymbol{r}',\boldsymbol{r},-i\omega_n). \quad \text{(A22)}$$

The LDOS shown in Fig. 3 is obtained by the analytic continuation of the diagonal elements of the single-particle Green's function as $G_{ii}(\boldsymbol{r},\boldsymbol{r}',i\omega_n \to \omega + i\delta)$ with δ being an infinitesimally small positive number.

[1] P. Fulde and R. A. Ferrell, Phys. Rev. **135**, A550 (1964).
[2] A. I. Larkin and Y. N. Ovchinnikov, Zh. Eksp. Teor. Fiz. **47**, 1136 (1964) [Sov. Phys. JETP **20**, 762 (1965)].
[3] Y. Matsuda and H. Shimahara, J. Phys. Soc. Jpn. **76**, 051005 (2007).
[4] S. Kitagawa, G. Nakamine, K. Ishida, H. S. Jeevan, C. Geibel, and F. Steglich, Phys. Rev. Lett. **121**, 157004 (2018).
[5] C.-w. Cho, J. H. Yang, N. F. Q. Yuan, J. Shen, T. Wolf, and R. Lortz, Phys. Rev. Lett. **119**, 217002 (2017).
[6] S. Kasahara, Y. Sato, S. Licciardello, M. Čulo, S. Arsenijević, T. Ottenbros, T. Tominaga, J. Böker, I. Eremin, T. Shibauchi, J. Wosnitza, N. E. Hussey, and Y. Matsuda, Phys. Rev. Lett. **124**, 107001 (2020).
[7] S. Yonezawa, S. Kusaba, Y. Maeno, P. Auban-Senzier, C. Pasquier, K. Bechgaard, and D. Jérome, Phys. Rev. Lett. **100**, 117002 (2008).
[8] H. Mayaffre, S. Krämer, M. Horvatic, C. Berthier, K. Miyagawa, K. Kanoda, and V. F. Mitrovic, Nat. Phys. **10**, 928 (2014).
[9] K. Kumagai, H. Shishido, T. Shibauchi, and Y. Matsuda, Phys. Rev. Lett. **106**, 137004 (2011).
[10] M. Kenzelmann, Rep. Prog. Phys. **80**, 034501 (2017).

[11] A. B. Vorontsov and J. A. Sauls, Phys. Rev. Lett. **98**, 045301 (2007).
[12] K. Aoyama, Phys. Rev. B **89**, 140502(R) (2014).
[13] J. J. Wiman and J. A. Sauls, J. Low Temp. Phys. **184**, 1054 (2016).
[14] L. V. Levitin, B. Yager, L. Sumner, B. Cowan, A. J. Casey, J. Saunders, N. Zhelev, R. G. Bennett, and J. M. Parpia, Phys. Rev. Lett. **122**, 085301 (2019).
[15] A. J. Shook, V. Vadakkumbatt, P. Senarath Yapa, C. Doolin, R. Boyack, P. H. Kim, G. G. Popowich, F. Souris, H. Christani, J. Maciejko, and J. P. Davis, Phys. Rev. Lett. **124**, 015301 (2020).
[16] M. Alford, J. A. Bowers, and K. Rajagopal, Phys. Rev. D **63**, 074016 (2001).
[17] R. Casalbuoni and G. Nardulli, Rev. Mod. Phys. **76**, 263 (2004).
[18] R. Anglani, R. Casalbuoni, M. Ciminale, N. Ippolito, R. Gatto, M. Mannarelli, and M. Ruggieri, Rev. Mod. Phys. **86**, 509 (2014).
[19] A. Sedrakian, Phys. Rev. C **63**, 025801 (2001).
[20] A. A. Isayev, Phys. Rev. C **65**, 031302(R) (2002).
[21] T.-G. Lee, R. Yoshiike, and T. Tatsumi, JPS Conf. Proc. **20**, 011006 (2018).
[22] M. W. Zwierlein, A. Schirotzek, C. H. Schunck, and W. Ketterle, Science **311**, 492 (2006).
[23] G. B. Partridge, W. Li, R. I. Kamar, Y.-a. Liao, and R. G. Hulet, Science **311**, 503 (2006).
[24] G. B. Partridge, W. Li, Y. A. Liao, R. G. Hulet, M. Haque, and H. T. C. Stoof, Phys. Rev. Lett. **97**, 190407 (2006).
[25] S. Nascimbène, N. Navon, K. J. Jiang, L. Tarruell, M. Teichmann, J. McKeever, F. Chevy, and C. Salomon, Phys. Rev. Lett. **103**, 170402 (2009).
[26] Y.-a. Liao, A. S. C. Rittner, T. Paprotta, W. Li, G. B. Partridge, R. G. Hulet, S. K. Baur, and E. J. Mueller, Nature (London) **467**, 567 (2010).
[27] M. C. Revelle, J. A. Fry, B. A. Olsen, and R. G. Hulet, Phys. Rev. Lett. **117**, 235301 (2016).
[28] T. Mizushima, K. Machida, and M. Ichioka, Phys. Rev. Lett. **94**, 060404 (2005).
[29] H. Hu and X.-J. Liu, Phys. Rev. A **73**, 051603(R) (2006).
[30] X.-J. Liu, H. Hu, and P. D. Drummond, Phys. Rev. A **75**, 023614 (2007).
[31] D. T. Son and M. A. Stephanov, Phys. Rev. A **74**, 013614 (2006).
[32] D. E. Sheehy and L. Radzihovsky, Ann. Phys. (NY) **322**, 1790 (2007).
[33] A. Bulgac and M. M. Forbes, Phys. Rev. Lett. **101**, 215301 (2008).
[34] M. M. Parish, F. M. Marchetti, A. Lamacraft, and B. D. Simons, Nat. Phys. **3**, 124 (2007).
[35] T. Mizushima, M. Ichioka, and K. Machida, J. Phys. Soc. Jpn. **76**, 104006 (2007).
[36] K. Machida, T. Mizushima, and M. Ichioka, Phys. Rev. Lett. **97**, 120407 (2006).
[37] G. Orso, Phys. Rev. Lett. **98**, 070402 (2007).
[38] H. Hu, X.-J. Liu, and P. D. Drummond, Phys. Rev. Lett. **98**, 070403 (2007).
[39] X. W. Guan, M. T. Batchelor, C. Lee, and M. Bortz, Phys. Rev. B **76**, 085120 (2007).
[40] M. M. Parish, S. K. Baur, E. J. Mueller, and D. A. Huse, Phys. Rev. Lett. **99**, 250403 (2007).
[41] L. O. Baksmaty, H. Lu, C. J. Bolech, and H. Pu, Phys. Rev. A **83**, 023604 (2011).
[42] L. O. Baksmaty, H. Lu, C. J. Bolech, and H. Pu, New J. Phys. **13**, 055014 (2011).
[43] N. Yoshida and S.-K. Yip, Phys. Rev. A **75**, 063601 (2007).
[44] X.-J. Liu, H. Hu, and P. D. Drummond, Phys. Rev. A **76**, 043605 (2007).
[45] G. J. Conduit, P. H. Conlon, and B. D. Simons, Phys. Rev. A **77**, 053617 (2008).
[46] Y. Yanase, Phys. Rev. B **80**, 220510(R) (2009).
[47] T. Yoshida and Y. Yanase, Phys. Rev. A **84**, 063605 (2011).
[48] R. Yoshii, S. Takada, S. Tsuchiya, G. Marmorini, H. Hayakawa, and M. Nitta, Phys. Rev. B **92**, 224512 (2015).
[49] T. K. Koponen, T. Paananen, J.-P. Martikainen, M. R. Bakhtiari, and P. Törmä, New J. Phys. **10**, 045014 (2008).
[50] M. W. Zwierlein, C. H. Schunck, A. Schirotzek, and W. Ketterle, Nature (London) **442**, 54 (2006).
[51] F. Gygi and M. Schlüter, Phys. Rev. B **43**, 7609 (1991).
[52] M. Takahashi, T. Mizushima, M. Ichioka, and K. Machida, Phys. Rev. Lett. **97**, 180407 (2006).
[53] K. M. Suzuki, T. Mizushima, M. Ichioka, and K. Machida, Phys. Rev. A **77**, 063617 (2008).
[54] C. Caroli, P. D. Gennes, and J. Matricon, Phys. Lett. **9**, 307 (1964).
[55] N. Hayashi, T. Isoshima, M. Ichioka, and K. Machida, Phys. Rev. Lett. **80**, 2921 (1998).
[56] K. Machida and H. Nakanishi, Phys. Rev. B **30**, 122 (1984).
[57] T. Mizushima and K. Machida, Philos. Trans. R. Soc., A **376**, 20150355 (2018).
[58] Y. Ohashi and S. Takada, J. Phys. Soc. Jpn. **65**, 246 (1996).
[59] Y. Sagi, T. E. Drake, R. Paudel, R. Chapurin, and D. S. Jin, Phys. Rev. Lett. **114**, 075301 (2015).
[60] Y. Ohashi, J. Phys. Soc. Jpn. **71**, 2625 (2002).
[61] H. Shimahara, J. Phys. Soc. Jpn. **67**, 1872 (1998).
[62] R. Sensarma, M. Randeria, and T.-L. Ho, Phys. Rev. Lett. **96**, 090403 (2006).